Coordination Polymers

DOI: 10.1002/ange.200500207

A Synthetic Zwitterionic Water Channel: Characterization in the Solid State by X-ray Crystallography and NMR Spectroscopy**

Zhaofu Fei, Dongbin Zhao, Tilmann J. Geldbach, Rosario Scopelliti, Paul J. Dyson, Sasa Antonijevic,* and Geoffrey Bodenhausen*

Bio-inspired supramolecular frameworks are of both fundamental value as models and of practical importance in areas such as materials science, catalysis, and molecular electronics.[1–3] Many of these synthetic materials are constructed from metal ions as connectors and ligands as linkers, and are referred to as coordination polymers.[4] Porous materials are of particular interest, as the nanosized cavities lead to novel phenomena, with applications in separation, storage, and catalysis. In this respect, attempts to generate synthetic water channels that mimic aquaporin water channels[5] have met with some success.[6–10] Here we describe a zwitterionic, helical tube of nanodimensions that to some extent mimics aquaporin, and provide a detailed study of the water incorporated inside the channel over a wide temperature range by solid-state ^{2}H NMR spectroscopy.

Reaction of the carboxy-functionalized imidazolium salt *N*,*N*′-diacetic acid imidazolium bromide[11] with zinc in aqueous solution affords zwitterionic coordination polymer **1** in crystalline form. The structure of **1** was characterized by single-crystal X-ray diffraction at 140 K and is shown in Figure 1. To ensure that the encapsulated water does not undergo any structural changes at ambient temperature, the structure was also determined at 293 K (see Supporting Information). The macrostructure is formed from $ZnBr(H_2O)$ units linked by bridging dicarboxylate anions, which assemble into helical channels and appear to be supported by weak π-stacking interactions between the imidazolium moieties and by intrahelical hydrogen bonds. The strongest hydrogen bonds stem from contacts of the carboxy oxygen atom O2 to H3 and H6 in the next layer. Two molecules constitute a full cycle within the helix with distances between the layers of 6.234 Å. The cavity of the channel is occupied by water molecules, which form a one-dimensional chain with distances between the oxygen atoms of 3.157 Å.

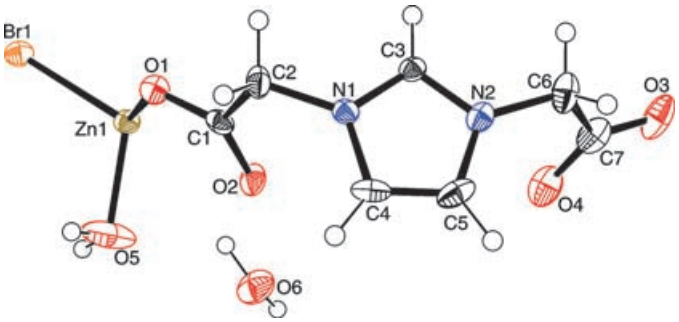

Figure 1. Structure of the asymmetric unit of **1** (ORTEP plot; ellipsoids are drawn at the 50% probability level). Selected bond lengths [Å] and angles [°]: Zn1–Br1 2.3677(6), Zn–O1 1.977(2), Zn–O4 1.983(3), Zn–O5 2.014(3), C1–O1 1.270(4), C1–O2 1.243(4), C7–O3 1.199(5), C7–O4 1.287(5); O1-C1-O2 124.9(3), O3-C7-O4 126.2(4), Br1-Zn1-O1 109.73(7), Br1-Zn1-O5 111.0(1), Br1-Zn1-O4 114.88(8), O1-Zn1-O5 110.4(1), O1-Zn1-O4 117.1(1), O4-Zn1-O5 92.5(2).

The coordination sphere around the zinc anion in **1** is best described as a distorted tetrahedron with angles between 92.5(2) and 117.1(1)°. Zinc–oxygen bond lengths lie between 1.997(2) and 2.014(3) Å, and both angles and bond lengths are in good agreement with those of comparable zinc dicarboxylate polymers.[12]

The helices are packed in a hexagonal-based array with pronounced interhelical hydrogen bonding (Figure 2b). Each asymmetric unit has five contacts shorter than 3 Å to neighboring helices, which arise from medium-strength interactions from O1 and O3 and weaker contacts from the bromide ligands. The hydrogen atoms H61 and H62 of the encapsulated water molecule are engaged in strong hydrogen

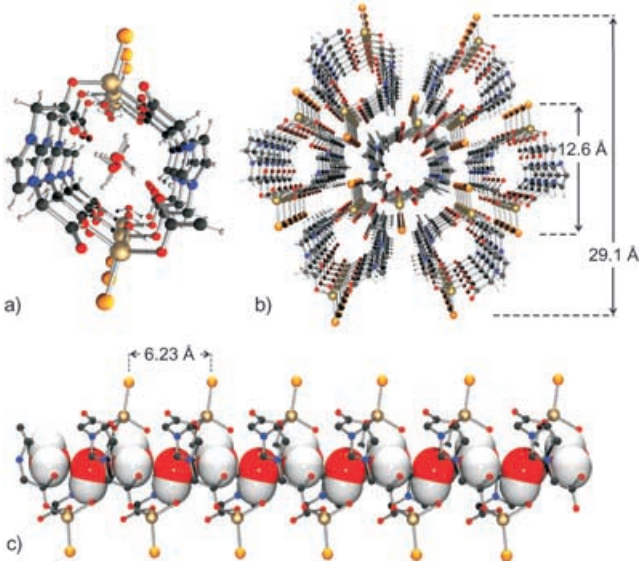

Figure 2. a) View into the helical tube of **1** with the one-dimensional water chain in the center. b) View into the helical tube of **1** with the free water molecules removed for clarity. c) View along the *y* axis showing the encapsulated water drawn with van der Waals radii. Hydrogen atoms on the imidazolium moiety have been omitted for clarity.

[*] Dr. Z. Fei, D. Zhao, Dr. T. J. Geldbach, Dr. R. Scopelliti, Prof. Dr. P. J. Dyson, Dr. S. Antonijevic, Prof. Dr. G. Bodenhausen
Institut des Sciences et Ingénierie Chimiques
Ecole Polytechnique Fédérale de Lausanne, EPFL-BCH
1015 Lausanne (Switzerland)
Fax: (+41) 21-693-9885
E-mail: paul.dyson@epfl.ch
Sasa.Antonijevic@epfl.ch

[**] We thank the EPFL and Swiss National Science Foundation for financial support and Dr. P. G. Anil Kumar at the ETH (Zürich) for solution diffusion measurements.

Supporting information for this article is available on the WWW under http://www.wiley-vch.de/home/angewandte/ or from the author.

bonding to oxygen atoms O2 and O4 on the inner wall of the tube, both of which bear a delocalized negative charge. As a result of these quite strong interactions the oxygen atoms of the water molecules are in relatively close contact and are not bridged by a hydrogen atom. A summary of the more important hydrogen-bonding interactions (< 3 Å) is given in Table 1.

Table 1: Hydrogen-bonding distances [Å] in **1**.

Interhelical contacts		Intrahelical contacts		Contacts from free water	
Br–H2	2.952	O2–H3	2.461	O2–H62	1.728
Br–H4	2.823	O2–H6	2.908	O4–H61	2.194
Br–H6	2.960			O5–H61	2.261
O1–H2	2.405				
O3–H5	2.353				

The inner dimensions of the imidazolium–zinc channel are 5.656 and 6.515 Å between adjacent oxygen atoms O2 and O4, respectively, resulting in a cavity of about 2.656×3.513 Å^2 if van der Waals radii are taken into account.[13]

In the mass spectrum, no evidence of aggregates is observed, and pulsed-field-gradient spin-echo (PGSE) diffusion measurements on **1** in D_2O solution confirmed that **1** exists as a monomer in solution. The estimated diffusion coefficient is 5.65×10^{-10} m^2 s^{-1}, which corresponds to a hydrodynamic radius of about 3.8 Å. This value is in good agreement with that of 3.6 Å for the analogous zwitterionic imidazolium carboxylate (see Supporting Information).

To gain a more comprehensive understanding of the properties of the one-dimensional water chain and to characterize the local mobility of the two different types of water molecules in the helix, **1** was studied by solid-state ^{13}C and ^{2}H NMR spectroscopy. Figure 3 shows the ^{13}C cross-polarized (CP) magic-angle spinning (MAS) NMR spectrum of **1**. Seven nicely resolved resonance signals are associated with seven crystallographically different carbon atoms in the asymmetric unit cell as follows: C1 and C7 at $\delta = 174.07$ and 175.46 ppm; C2 and C6 at $\delta = 53.56$ and 54.78 ppm; C3 at $\delta = 139.67$; and C4 and C5 at $\delta = 125.07$ and 125.77 ppm. The linewidths (full width at half-height, FWHH) of C1 and C7 are only 30 Hz and could be obtained by very accurate

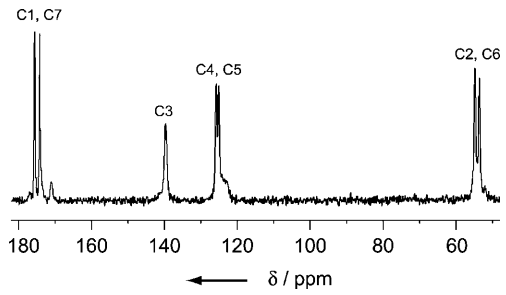

Figure 3. ^{13}C CPMAS NMR spectrum of **1** displays seven resolved resonance signals that are assigned to seven crystallographically different carbon atoms in the asymmetric unit cell. The spectrum is the result of averaging 8000 transients.

adjustment of the magic angle (better than $\pm 0.004°$).[14,15] Such narrow ^{13}C resonances suggest that the helical framework structure of this coordination polymer experiences very little structural disorder, if any.[16] The linewidths of the other carbon atoms are in the range of 50–80 Hz, and are due in part to residual dipolar splittings (or second-order quadrupole–dipole cross-terms) to neighboring ^{14}N atoms.[17–19] The assignment of the chemical shifts of pairs of chemically identical carbon atoms is not feasible from the ^{13}C CPMAS spectrum alone.

Understanding the motional behavior of water molecules that constitute a one-dimensional chain may prove important for the rationalization of various biological processes. To distinguish the two different types of water molecules in **1** and individually examine their motional behavior, they were replaced by D_2O by recrystallization of **1** from heavy water to give the deuterated material **1-D**. The water content of **1-D** amounts to 98% of the theoretical value, as determined by thermogravimetric analysis.

Motional disorder can be readily probed by static and MAS ^{2}H NMR experiments over a wide range of correlation rates, namely, 10^2 s$^{-1} < k < 10^9$ s^{-1}.[20–22] The high-resolution ^{2}H MAS spectra of **1-D** in Figure 4 show three resonances at isotropic chemical shifts $\delta_{iso} = 2.19$, 3.24, and 7.09 ppm. The very narrow resonance at $\delta = 2.19$ ppm (marked with $*$) is assigned to residual [D_6]acetone, which was used in the preparation of **1-D**. This resonance, which in comparison to the other two resonances displays only a center band, makes a negligible contribution to the overall signal. The other two resonances are assigned to water molecules and exhibit different linewidths due to structural disorder of water molecules and/or motional broadening. The considerable difference in the local magnetic fields, reflected in a relatively large difference in isotropic chemical shift, is due to the very different electronic environments of the two types of water molecules. One is coordinated to zinc ($\delta = 7.09$ ppm), whereas the other is located in the middle of the channel ($\delta =$ 3.24 ppm).

Variable-temperature ^{2}H MAS NMR spectra of **1-D** reveal changes in the linewidths of the ^{2}H resonances of both types of water molecules and thus indicate their mobility. Increasing temperature results in line narrowing, and this suggests that both types of water molecules move in the fast motional regime, typically $k \geq 10^7$ s^{-1}.[21–23] Decreasing the temperature leads to line broadening, and the linewidths observed at 246 K for both water resonances are so large that spinning sidebands are barely observable. The rate of the motions in this intermediate regime is typically in the range 10^7 s$^{-1} \geq k \geq 10^4$ s^{-1}. Figure 4b shows a ^{2}H MAS spectrum of **1-D** that was exposed to high vacuum (0.01 mbar) for 4 min. The loss of about 10% of the total amount of water indicates that water molecules can be relatively easily removed from the channel. Both deuterium resonances arising from deuterons of water molecules in Figure 4b are narrower than in Figure 4a. The narrowing of the resonance at $\delta = 3.24$ ppm is more pronounced, most probably due to increased mobility of the free water molecules.

It is expected that water molecules bound to zinc have restricted motional freedom and undergo a reorientational

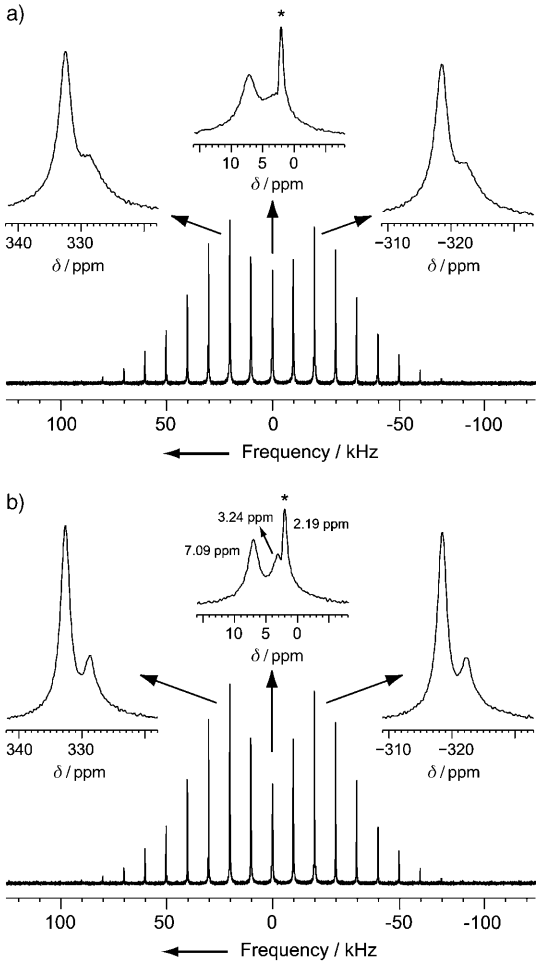

Figure 4. ^{2}H MAS NMR spectra of **1-D**: a) as synthesized and b) treated under high vacuum (0.01 mbar) for 4 min. The center band of (b) displays three resolved signals: two water molecules at $\delta = 7.09$ and 3.24 ppm and a narrow signal at $\delta = 2.19$ ppm (marked with *) originating from traces of [D_6]acetone. The spectra are the result of averaging 640 transients. A line broadening of 10 Hz was applied to both spectra.

motion which is often a 180° flip around the DOD bisector.[24] The free water in the channel, on the other hand, is expected to have more motional freedom, even to the extent of fast isotropic tumbling.[20] Both types of motion lead to averaging of the quadrupolar interaction. The former yields an averaged quadrupolar interaction that is comparable in magnitude to the quadrupolar interaction in the absence of the motion. The latter results in a more pronounced averaging of the quadrupolar interaction, and in extreme cases only a tiny residual quadrupolar interaction is observed. Note that not only reorientation and/or tumbling of the actual deuteron results in averaging of the quadrupolar interaction, but molecular motions of the nearest neighbors can also introduce a time-dependent electric field gradient and hence a time-dependent quadrupolar interaction.

Figure 5 shows the experimental ^{2}H NMR spectra of **1-D** (solid line) recorded at different temperatures under static conditions. They display a complex lineshape resulting from an overlap of several resonances. The narrow resonance at

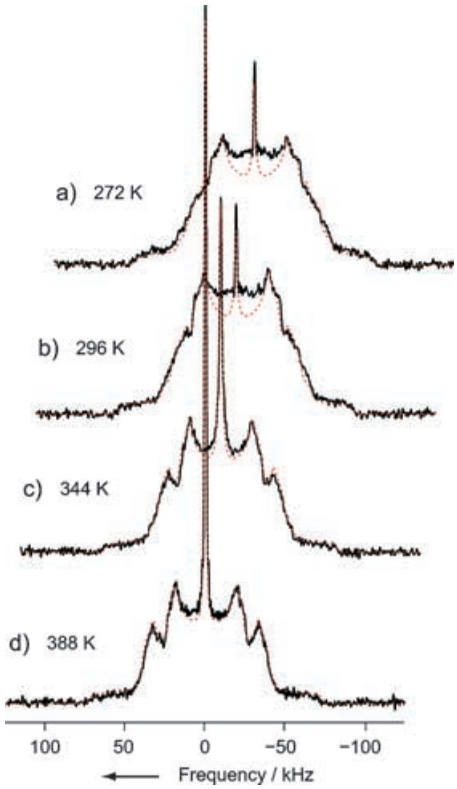

Figure 5. Experimental (solid) and simulated (dashed) static ^{2}H NMR spectra of **1-D** recorded as a function of temperature. The narrow signal at $\delta = 2.19$ ppm in a) and b) purely arises from residual [D_6]acetone. The spectra are the result of averaging 640 transients.

$\delta = 2.19$ ppm in the two spectra at lower temperatures is assigned to traces of [D_6]acetone. This resonance is also present in the spectra recorded at higher temperatures, but here it overlaps with newly formed narrow resonances, as shown in Figure 5c and d. The broad features of the spectra resemble superposition of two deuterium powder patterns. The narrower powder pattern has $\delta_{iso} = 3.24$ ppm, while the broader powder pattern has $\delta_{iso} = 7.09$ ppm, as found from the spectra in Figure 4. They are assigned to free and bound water molecules, respectively. Each powder pattern can be represented by an averaged quadrupolar coupling constant C_Q and an asymmetry parameter η_Q. Simulated spectra obtained by using the averaged quadrupolar parameters listed in Table 2 are in a very good agreement with the experimental spectra (Figure 5). In the absence of motions, C_Q for deuterons of D_2O in solids is typically in the range $240 \geq C_Q \geq 180$ kHz.[25] Evidently, the quadrupolar interaction for the free water molecules is averaged to a greater extent. Bound-water

Table 2: Quadrupolar parameters C_Q and η_Q of **1-D** as determined from static ^{2}H NMR spectra recorded at different temperatures.

T [K]	Bound water ($\delta_{iso} = 7.09$ ppm)		Free water ($\delta_{iso} = 3.24$ ppm)	
	C_Q [kHz]	η_Q	C_Q [kHz]	η_Q
272	98.4	0.14	64.5	0.16
296	96.7	0.12	62.9	0.15
344	96.7	0.09	60.5	0.14
388	96.7	0.09	57.6	0.11

deuterons experience a slight decrease of averaged quadrupolar parameters with increasing temperature, which indicates that there is little change in motional freedom. However, the significant change in C_Q and η_Q for free-water deuterons is indicative of a significant change in motional freedom of these water molecules. Curiously, neither of the two averaged powder patterns corresponds to that which would arise for 180° flips around the DOD bisector, which normally results in averaged values of $\eta_Q \approx 1$.[24]

The intensity ratio of the two powder patterns at lower temperatures is estimated to be 1:1, while at higher temperatures (Figure 5c, d) the intensity of the narrower pattern (free water molecules) decreases by conversion to a newly formed narrow resonance. This "sudden" formation of a new narrow resonance is observed between 336 and 345 K. It has a linewidth typical for water undergoing isotropic motion and cannot result only from an increased rate of motion or deuterium transfer, that is, in the fashion of a proton (deuteron) wire. The observed increase in motional freedom might occur either due to some structural change or to water "rattling" (i.e., diffusing into unoccupied positions) through the channel. A structural change could be expected to result in an increase of motional freedom for *all* free water molecules, but this was not observed. On the other hand, unoccupied water sites represent an opportunity for some water molecules to undergo a translational "hopping" motion. We find that any changes observed in ^{2}H spectra of **1-D** exposed to temperatures in the range from 240 to 390 K are reversible. In samples of **1-D** with 100% water content, where there are no vacant sites in the helix, another very sharp resonance (FWHH of 5 Hz) at $\delta = 5.0$ ppm is observed at 353 K (see Supporting Information). This very narrow resonance is characteristic of water that tumbles very rapidly and was therefore assigned to adsorbed or surface water. It is not clear if these water molecules are released from the channel as a direct consequence of water transport through the channel, as found in other one-dimensional water-channel systems,[26–28] or due to a rather unlikely diffusion process through the "walls" of the nanotubes. In samples with less than 100% water content, water molecules do not appear to leave the tubes when the temperature increases, but move along the vacant sites. The existence of vacant sites was shown to be critical for diffusion processes observed in zeolites containing one-dimensional water channels.[27]

Studies on helical zinc complexes of carboxylic acids have been previously reported,[29,30] including conducting helical polymers,[31] of which zwitterionic polymers are of special interest.[32] In this work, however, the water molecules in the helical channel have been studied by ^{2}H NMR spectroscopy, and it was possible to differentiate the two different types of water molecules. One is assigned to deuterons of free water molecules found in the middle of the channels, while the other corresponds to water coordinated to zinc. Both undergo fast motions ($k \geq 10^7\ s^{-1}$) at room temperature. The quadrupolar interaction of free-water deuterons in **1-D** is scaled to a greater extent, and this indicates different motional behavior than for the bound water molecules. Furthermore, the motional freedom of free water molecules increases with increasing temperature, since the quadrupolar parameters decrease, while they remain the same for the bound-water deuterons. Neither of the two deuterium powder patterns corresponds to simple 180° flips around the DOD bisector. Partial displacement of water molecules from the channel seems to be a process with a low activation energy barrier, since a significant fraction of the water molecules can be removed by short exposure to high vacuum. The change in the motional behavior of a fraction of the free water molecules in **1-D** that occurs between 336 and 345 K results in a dramatic averaging of C_Q. This is most probably due the water "rattling" along the channel, permitted by the existence of vacant water positions, in addition to already existing motional degrees of freedom. Proton (deuteron) transfer can be ruled out as a source of such an observation. The very narrow peak at $\delta = 5.0$ ppm observed at 353 K for **1** without water vacancies is related to water molecules that are delivered to the outside of the channels and have a liquidlike motional behavior. It is likely that these water molecules either diffuse out of the channels or escape as a result of water transfer through the channel. Finally, a possible exchange of deuterons between two different types of water molecules may occur, but on a timescale with a rate constant that is much smaller than the quadrupolar splitting.

It is interesting to compare **1** to other systems that contain water in a confined channel. For example, aquaporin water channels (AQP1) are composed of an hourglass structure with a narrowest constriction of 2.8 Å (Figure 6); the narrowest gap in the channel of **1** is 2.656 Å.

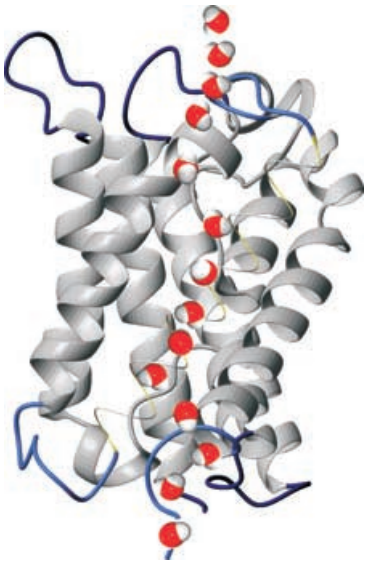

Figure 6. Schematic representation of water flow through an aquaporin channel.

Although **1** resembles an aquaporin channel in that the water molecules form a single file and the diameter of the tube is of approximately the same size as the narrowest part of the pore in the protein, there are also fundamental differences. Owing to the presence of strong hydrogen bonds between the hydrogen atoms of the encapsulated water molecules and oxygen atoms of the inner wall, both water

hydrogen atoms point towards the wall of the tube, rather than to neighboring water molecules. In contrast, each water molecule in aquaporin water channels forms one hydrogen bond with the wall of the protein and one with an adjacent water molecule. Furthermore, the water molecules in the aquaporin channel undergo a fliplike motion while passing through the pore. This change in orientation is crucial for proton exclusion and it thereby preserves the electrochemical potential across the cell membrane.[33] Owing to the uniformity of the zwittertube, no comparable conformational change is observed along the chain of water molecules. As the wall of the nanotube consists of zwitterionic residues, interactions between the water molecules are much stronger than in the biological system, where dipole–dipole interactions dominate. This has implications with respect to the efficiency with which the channel can transport water. It was previously demonstrated in carbon nanotubes that the high affinity of water molecules to charged moieties significantly decreases their mobility.[34] While the rate of water transport at room temperature in aquaporin is on the order of one molecule per nanosecond,[35] it is believed to be slower in the zwittertube.

Experimental Section

Synthesis of **1**: A mixture of elemental zinc (1.50 g, 23 mmol) and **2** (2.65 g, 10 mmol) in water (20 mL) was stirred for 10 days at room temperature, after which time no further evolution of hydrogen gas could be observed. The mixture was filtered, and the filtrate concentrated to half of its volume and left at room temperature for seven days to afford big colorless crystals. Yield: 96%. ESI-MS: *m/z*: 328 $[M-2H_2O]^+$, 344 $[M-H_2O]^+$; ^{1}H NMR (400.1 MHz, D_2O): $\delta =$ 8.68 (s, 1H), 7.36 (s, 2H), 4.80 ppm (s, 4H); ^{13}C NMR (100.6 MHz, D_2O): $\delta = 172.33, 137.18, 123.17, 51.94$ ppm; IR: $\tilde{\nu} = 3150, 3108, 3017, 2950, 1622, 1589, 1565, 1437, 1397, 1298, 1177, 1162, 1101, 971, 765, 681$ cm^{-1}; elemental analysis (%) calcd for $C_7H_{11}BrN_2O_6Zn$ (364.46): C 23.07, H 3.04, N 7.69; found: C 23.11, H 3.07, N 7.75.

Synthesis of **1-D**: A sample of **1** was dissolved in D_2O followed by immediate removal of the solvent at low temperature (2–5 °C) to afford **1-D**. The solid was washed with [D_6]acetone to remove residual water absorbed on the surface. The water content was determined to be 98% of the theoretical value by thermogravimetric analysis and was confirmed by elemental analysis. Unwanted exchange of protons at C3 was observed when the sample of **1-D** was prepared at room temperature with slow evaporation of the solvent. The D3 deuteron of this material results in an additional ^{2}H NMR resonance at $\delta =$ 9.1 ppm (see Supporting Information), which makes interpretation of the NMR spectra more complicated. Similarly, if the reaction of the acid with elemental zinc was carried out in D_2O, unwanted exchange of H2, H3, and H6 is observed.

Crystallography: Single crystals of **1** were measured on a KUMA CCD diffractometer. Data reduction was performed with CrysAlis RED.[36] Structure solution and refinement were performed with the SHELX97 software package;[37] graphical representations of the structures were made with ORTEP32.[38] Structures were solved by direct methods and successive interpretation of the difference Fourier maps, followed by full-matrix least-squares refinement (against F^2). An empirical absorption correction (DELABS)[39] was applied. All non-hydrogen atoms were refined anisotropically. Hydrogen atoms on the imidazolium moiety were placed in their geometrically generated positions and refined with a riding model. Water hydrogen atoms were located on the Fourier map and refined by using the HTAB command with a fixed O–H distance of 0.98 Å and with an additional H···H restraint (1.60 Å) by using the DFIX command in SHELX97.

Crystal data of $C_7H_7BrN_2O_4Zn\cdot 2H_2O$ (**1**): Crystal dimensions $0.19\times0.10\times0.06$ mm^3, monoclinic, space group $P2(1)/n$, $a =$ 9.9025(8), $b = 6.2345(4)$, $c = 19.3319(15)$ Å, $\beta = 99.314(7)°$, $V =$ 1177.76(15) Å^3, $\rho_{calcd} = 2.055$ Mg m^{-3}, $Z = 4$, $\mu = 5.496$ mm^{-1}, $\theta_{max} =$ 3.44 to 25.03, $Mo_{K\alpha}$ radiation ($\lambda = 0.71070$ Å), $T = 140$ K, $F(000) =$ 720, total reflections 6384, independent reflections 1971 ($R_{int} =$ 0.0400), observed data 1677 ($I > 2\sigma(I)$). The final anisotropic full-matrix least-squares refinement on F^2 for 166 variables converged at $R_1 = 0.0271$ and $wR_2 = 0.0636$ with a GOF of 1.061. CCDC-251434 contains the supplementary crystallographic data for this paper. These data can be obtained free of charge from The Cambridge Crystallographic Data Centre via www.ccdc.cam.ac.uk/data_request/cif.

Solid-state NMR measurements: Spectra were recorded on a Bruker Avance 400 spectrometer equipped with a wide-bore 9.4 T magnet, operating at a Larmor frequency of $\nu_0 = 61.4$ MHz for ^{2}H ($S = 1$) and 100.6 MHz for ^{13}C ($S = 1/2$). Cross-polarized (CP) ^{13}C{^{1}H} MAS NMR spectra were recorded with a standard Bruker 2.5 mm CPMAS probe with a spinning rate of 30 kHz, a ^{1}H radio-frequency (RF) field strength of 85 kHz, a contact time of 1 ms, and a recycle interval of 3 s. The best performance of TPPM proton decoupling during acquisition was obtained with pulse widths of 3.9 μs at 100 kHz ^{1}H RF field and a phase difference between two successive pulses of 35°. The magic angle was adjusted first by minimizing the residual quadrupolar splitting in the rotor-synchronized ^{2}H MAS spectrum of α-oxalic acid [D_6]dehydrate.[12] The subsequent fine adjustment was carried out by maximizing the height of the ST_1-CT shifted-echo signal in a one-dimensional STMAS experiment.[12,15] Static and MAS deuterium spectra were recorded with a Bruker 4 mm MAS probe. A 500 W RF amplifier was used to give a ^{2}H 90° pulse duration of 2.9 μs. The static wide-line deuterium powder patterns were recorded by using "Exorcycled" quadrupolar echo pulse sequence to avoid distortions due to chemical shift anisotropy (CSA).[40] The variable-temperature ^{2}H MAS experiments were performed at a spinning rate of 10 kHz. A recycle interval of 1 s was appropriate for all deuterium resonances. The temperature was calibrated by using $Pb(NO_3)_2$ as a chemical shift thermometer.[41] Chemical shifts are reported in ppm relative to adamantane (high-frequency resonance at $\delta = 38.56$ ppm) for ^{13}C and TMS for ^{2}H. The frequency-domain simulated spectra were produced by a home-written program which does not take finite pulse duration effects into account, and does not include any time dependence of the quadrupolar interaction.[42]

Received: January 19, 2005
Revised: April 25, 2005
Published online: August 1, 2005

Keywords: coordination polymers · helical structures · NMR spectroscopy · supramolecular chemistry · water channels

[1] C. T. Kresge, M. E. Leonowicz, W. J. Roth, J. C. Vartuli, J. S. Beck, *Nature* **1992**, *359*, 710–712.
[2] R. S. Meissner, J. Rebek, Jr., J. de Mendoza, *Science* **1995**, *270*, 1485–1488.
[3] S. Mann, *Biomimetic Materials Chemistry*, VCH, New York, 1996.
[4] S. Kitagawa, R. Kitaura, S.-i. Noro, *Angew. Chem.* **2004**, *116*, 2388–2430; *Angew. Chem. Int. Ed.* **2004**, *43*, 2334–2375.
[5] P. Agre, *Angew. Chem.* **2004**, *116*, 4377–4390; *Angew. Chem. Int. Ed.* **2004**, *43*, 4278–4290.
[6] V. Videnova-Adrabinska, *J. Mater. Chem.* **2002**, *12*, 2931–2935.
[7] L. E. Cheruzel, M. S. Pometun, M. R. Cecil, M. S. Mashuta, R. J. Wittebort, R. M. Buchanan, *Angew. Chem.* **2003**, *115*, 5610–5613; *Angew. Chem. Int. Ed.* **2003**, *42*, 5452–5455.

[8] P. S. Sidhu, K. A. Udachin, J. A. Ripmeester, *Chem. Commun.* **2004**, 1358 – 1359.
[9] B. Sreenivasulu, J. J. Vittal, *Angew. Chem.* **2004**, *116*, 5893 – 5896; *Angew. Chem. Int. Ed.* **2004**, *43*, 5769 – 5772.
[10] A. Mukherjee, M. K. Saha, M. Nethaji, A. R. Chakravarty, *Chem. Commun.* **2004**, 716 – 717.
[11] Prepared in an analogous method to the chloride salt, by using $BrCH_2CO_2Me$ and HBr in place of $ClCH_2CO_2Me$ and HCl, as described in Z. Fei, D. Zhao, T. J. Geldbach, R. Scopelliti, P. J. Dyson, *Chem. Eur. J.* **2004**, *10*, 4886 – 4893.
[12] a) N. J. Burke, A. D. Burrows, A. S. Donovan, R. W. Harrington, M. F. Mahon, C. E. Price, *Dalton Trans.* **2003**, 3840 – 3849; b) A. D. Burrows, R. W. Harrington, M. F. Mahon, C. E. Price, *J. Chem. Soc. Dalton Trans.* **2000**, 3845 – 3854.
[13] R. D. Shannon, *Acta Crystallogr. Sect. A* **1976**, *32*, 751 – 767.
[14] S. Antonijevic, G. Bodenhausen, *Angew. Chem.* **2005**, *117*, 2995 – 2998; *Angew. Chem. Int. Ed.* **2005**, *44*, 2935 – 2038.
[15] S. E. Ashbrook, S. Wimperis, *J. Magn. Reson.* **2002**, *156*, 269 – 281.
[16] D. Sakellariou, S. P. Brown, A. Lesage, S. Hediger, M. Bardet, C. A. Meriles, A. Pines, L. Emsley, *J. Am. Chem. Soc.* **2003**, *125*, 4376 – 4380.
[17] J. G. Hexem, M. H. Frey, S. J. Opella, *J. Am. Chem. Soc.* **1981**, *103*, 224 – 226.
[18] A. Naito, S. Ganapathy, C. A. McDowell, *J. Chem. Phys.* **1981**, *74*, 5393 – 5397.
[19] C. A. McDowell in *Encyclopedia of Nuclear Magnetic Resonance*, *Vol. 5* (Eds.: D. M. Grant, R. K. Harris), Wiley, Chichester, **1996**, p. 2901.
[20] M. J. Duer, H. He, W. Kolodziejski, J. Klinowski, *J. Phys. Chem.* **1994**, *98*, 1198 – 1204.
[21] J. H. Kristensen, G. L. Hoatson, R. L. Vold, *Solid State Nucl. Magn. Reson.* **1998**, *13*, 1 – 37.
[22] J. H. Kristensen, G. L. Hoatson, R. L. Vold, *J. Chem. Phys.* **1999**, *110*, 4533 – 4553.
[23] S. E. Ashbrook, S. Antonijevic, A. J. Berry, S. Wimperis, *Chem. Phys. Lett.* **2002**, *364*, 634 – 642.
[24] T. Chiba, *J. Chem. Phys.* **1963**, *39*, 947 – 953.
[25] L. G. Butler, T. L. Brown, *J. Am. Chem. Soc.* **1981**, *103*, 6541 – 6549.
[26] G. Hummer, J. C. Rasaiah, J. P. Noworyta, *Nature* **2001**, *414*, 188 – 190.
[27] P. Demontis, G. Stara, G. B. Suffritti, *J. Chem. Phys.* **2004**, *120*, 9233 – 9244.
[28] S. Nair, Z. Chowdhuri, I. Perla, D. A. Neumann, L. C. Dickinson, G. Tompsett, H-K. Jeong, M. Tsapatsis, *Phys. Rev. B* **2005**, *71*, 104301 – 104308.
[29] P. Jiang, Z. Guo, *Coord. Chem. Rev.* **2004**, *248*, 205 – 229.
[30] A. Erxleben, *Coord. Chem. Rev.* **2003**, *246*, 203 – 228.
[31] T. Hatano, A.-H. Bae, M. Takeuchi, N. Fujita, K. Kaneko, H. Ihara, M. Takafuji, S. Shinkai, *Angew. Chem.* **2004**, *116*, 471 – 475; *Angew. Chem. Int. Ed.* **2004**, *43*, 465 – 469.
[32] H. Terao, T. Sugawara, Y. Kita, N. Sato, E. Kaho, S. Takeda, *J. Am. Chem. Soc.* **2001**, *123*, 10468 – 10474.
[33] E. Tajkhorshid, P. Nollert, M. Ø. Jensen, L. J. W. Miercke, J. O'Connell, R. M. Stroud, K. Schulten, *Science* **2002**, *296*, 525 – 530.
[34] F. Zhu, K. Schulten, *Biophys. J.* **2003**, *85*, 236 – 244.
[35] a) M. Borgnia, S. Nielsen, A. Engel, P. Agre, *Annu. Rev. Biochem.* **1999**, *68*, 425 – 458; b) M. Ø. Jensen, E. Tajkhorshid, K. Schulten, *Biophys. J.* **2003**, *85*, 2884 – 2899.
[36] Oxford Diffraction Ltd, 68 Milton Park, Abingdon, OX144RX, UK, **2003**.
[37] G. M. Sheldrick, SHELX-97, Structure Solution and Refinement Package, Universität Göttingen, **1997**.
[38] L. J. Farrugia, *J. Appl. Crystallogr.* **1997**, *30*, 565.
[39] N. Walker, D. Stuart, *Acta Crystallogr. Sect. A* **1983**, *39*, 158 – 166.
[40] S. Antonijevic, S. Wimperis, *J. Magn. Reson.* **2003**, *164*, 343 – 350.
[41] A. Bielecki, D. P. Burum, *J. Magn. Reson. A* **1995**, *116*, 215 – 220.
[42] S. Antonijevic, S. Wimperis, *J. Chem. Phys.* **2005**, *122*, 044312 – 044314.

